Published in final edited form as:
Acta Biomater. 2015 February ; 13: 88–100. doi:10.1016/j.actbio.2014.11.002.

Injectable gelatin derivative hydrogels with sustained vascular endothelial growth factor release for induced angiogenesis

Zhe Li[a,b], **Tiejun Qu**[b,c], **Chen Ding**[b,d], **Chi Ma**[b], **Hongchen Sun**[e], **Shirong Li**[a,*], and **Xiaohua Liu**[b,*]

[a]Department of Plastic and Aesthetic Surgery, Southwest Hospital, Third Military Medical University, Chongqing, 400038, China

[b]Department of Biomedical Sciences, Texas A&M University Baylor College of Dentistry, Dallas, TX 75246, USA

[c]Department of Operative Dentistry & Endodontics, School of Stomatology, Fourth Military Medical University, Xi'an, 710032, China

[d]West China Hospital, West China School of Medicine, Sichuan University, Chengdu, 610041, China

[e]Department of Pathology, School of Stomatology, Jilin University, Changchun, 130021, China

Abstract

Injectable biomaterials are attractive for soft tissue regeneration because they are handled in a minimally invasive manner and can easily adapt to complex defects. However, inadequate vascularization of the injectable constructs has long been a barrier, leading to necrosis or volume reduction after implantation. In this work, we developed a three-step process to synthesize injectable gelatin-derived hydrogels that are capable of controlling growth factor delivery to induce angiogenesis. In our approach, tyramine was first introduced into gelatin chains to provide enzymatical crosslinking points for gel formation after injection. Next, heparin, a polysaccharide with binding domains to many growth factors, was covalently linked to the tyramine-modified gelatin. Finally, vascular endothelial growth factor (VEGF) was incorporated into the gelatin derivative by binding with the heparin in the gelatin derivative, and an injectable gel with controlled VEGF release was formed by an enzymatic catalytic reaction with hydrogen peroxide (H_2O_2) and horseradish peroxidase (HRP). The gelation time, mechanical properties and degradation of the gel was readily tailored by the gelatin concentration and the ratio of H_2O_2/HRP. Binding VEGF to heparin stabilizes this growth factor, protects it from denaturation and proteolytic degradation, and subsequently prolongs the sustained release. An *in vitro* release study

*Correspondence to: Xiaohua Liu, PhD, Assistant Professor, Department of Biomedical Sciences, Texas A&M University Baylor College of Dentistry, 3302 Gaston Ave., Dallas, TX 75246, Phone: 214-370-7007, Fax: 214-874-4538, xliu@bcd.tamhsc.edu; Shirong Li, Professor, Department of Plastic and Aesthetic Surgery, Southwest Hospital, Third Military Medical University, 30 Gaotanyan Main Street, Chongqing, 400038, China, Phone: +8602368765851, Fax: +8602368765851, sli1953@yahoo.com.

Author Disclosure Statement: No competing financial interests exist.

and bioactivity assay indicated that the VEGF was released in a sustained manner with high bioactivity for over 3 weeks. Furthermore, a chicken chorioallantoic membrane (CAM) assay and animal experiments were performed to evaluate *in vivo* bioactivity of the VEGF released from the hydrogels. After 5 days of incubation on CAM, the number of blood vessels surrounding the heparin-modified hydrogels was 2.4-fold increase than that of the control group. Deeper and denser cell infiltration and angiogenesis in the heparin-modified gelatin/VEGF gels were observed than in the controls after being subcutaneously injected in the dorsal side of the mice for 2 weeks. Interestingly, even without the incorporation of VEGF, the heparin-modified gelatin derivative still had the capability to induce angiogenesis to a certain degree. Our results suggest that the gelatin derivative/VEGF is an excellent injectable delivery system for induced angiogenesis of soft tissue regeneration.

Keywords

injectable hydrogel; gelatin; heparin; VEGF; angiogenesis; soft tissue regeneration

1. Introduction

Soft tissue defects resulting from traumatic injury, tumor resections, congenital defects or aging often lead to poor cosmesis, affect the emotional well-being of patients, and even impair function [1, 2]. According to the American Society of Plastic Surgeons (ASPS), 14.6 million cosmetic plastic surgery and 5.6 million reconstructive plastic surgery procedures were performed in the USA alone in 2012 [3]. While these treatments using autograft or allograft materials provide a reasonable degree of clinical success, they have significant drawbacks, including donor-site morbidity, unpredictable outcomes due to graft resorption over time, and allergic reactions [4]. Therefore, there is a clinical need for soft tissue substitutes.

Injectable fillers have been widely used as soft tissue substrates in recent years because they can be administrated in a minimally invasive manner and can easily adapt to complex defects [5-7]. A number of injectable commercial products are available on the market [5-8]. However, these materials act solely as fillers and often face limited longevity due to rapid resorption and the risk of potentially adverse reactions [8, 9]. A promising approach to solving these problems is the adoption of tissue engineering principles and the use of injectable biodegradable materials such as collagen, gelatin, fibrin, alginate, silk, and hyaluronic acid to guide the formation of new soft tissues [2]. Those natural injectable biomaterials are often presented in the form of hydrogels through physical or chemical crosslinking after implantation into the body, and have the advantages of excellent biocompatibility, degradability, and intrinsic cellular interaction. However, bioengineered grafts using injectable biomaterials alone often had inadequate neovascularization, leading to necrosis or volume reduction after implantation [10-12]. Vascularization is critical to the survival of engineered adipose tissue. In fact, insufficient vasculature has long been considered as one of the major barriers to regenerating large soft tissues for clinical application [2, 13, 14].

Several approaches have been reported to induce angiogenesis of adipose tissue [2, 15-18]. For example, co-cultivating human adipose tissue-derived mesenchymal stem cells with endothelial cells was tested to engineer vascularized soft tissues [18]. From a clinical point of view, however, the delivery of angiogenic growth factors, such as vascular endothelial growth factor (VEGF) and fibroblast growth factor 2 (FGF-2), is a simple and cost-effective strategy for vascularizing soft tissue grafts. Adipose tissue extract (ATE), which contains numerous angiogenic factors, was encapsulated in hyaluronan (HA) hydrogel and showed a strong induction in angiogenesis and adipogenesis both *in vitro* and *in vivo* [16, 19]. However, the ATE was simply mixed with the injectable HA, and the spatial-temporal delivery of the extract from the implant was not well controlled [19]. Collagen hydrogels containing FGF-2 encapsulated in gelatin microspheres were reported to better control FGF-2 delivery and facilitate the development of vascularized adipose tissue [17]. However, how to improve the mechanical properties of the collagen gel to better support the structure of the newly generated soft tissue has never been solved [17]. Overall, it is desirable to develop a new injectable scaffolding system with controlled angiogenic growth factor delivery for soft tissue regeneration.

In this study, we aimed to synthesize injectable gelatin-derivative hydrogels that are capable of controlling growth factor delivery and induced angiogenesis. We selected gelatin as the bulk biomaterial because gelatin is the product of the partial hydrolysis of collagen and is widely used as a drug delivery vehicle due to its excellent biodegradability and biocompatibility [15, 20, 21]. In contrast to collagen, gelatin is a denatured biopolymer and as a scaffolding material, it circumvents the concerns of the immunogenicity and pathogen transmission associated with collagen. Furthermore, the mechanical strength of the gelatin matrix can be readily tailored using the crosslinking density [21-23]. Several methods have been developed to prepare injectable gelatin gels through light, chemical, or enzymatical crosslinking [24-26]. Among these methods, enzymatical crosslinking is the most attractive because of its mild reaction process [27]. However, similar to other hydrogels, the release of growth factors from pure gelatin gel is a passive diffusion process, and therefore, has limited capability for controlled growth factor delivery. To solve this problem, we developed a new approach to incorporate both heparin and tyramine onto the gelatin chains in this study. Heparin was coupled to gelatin because heparin has binding domains with many growth factors, especially with VEGF, which is a heparin-binding glycoprotein [28, 29]. Binding of VEGF to heparin stabilizes this growth factor, protects it from denaturation and proteolytic degradation, and subsequently prolongs its sustained release [30-32]. Tyramine was included in the gelatin chains in order to provide enzymatical crosslinking points after injection [26, 33]. When this gelatin-derived solution is mixed with hydrogen peroxide (H_2O_2) and horseradish peroxidase (HRP), an enzymatic catalytic reaction takes places and forms an injectable hydrogel. We synthesized this gelatin derivative and evaluated its gelation process and mechanical properties. We also examined the release kinetics and bioactivity of VEGF released from the gel. Finally, a chicken embryo chorioallantoic membrane assay and animal experiments were performed to examine the potency of this injectable gelatin-derivative/VEGF for induced angiogenesis *in vivo*.

2. Materials and Methods

2.1 Materials

Gelatin (Type B, from bovine skin, 225 g Bloom, average molecular weight=50,000, Cat# G9391), heparin (sodium salt from porcine intestinal mucosa, MW ~ 17-19 kDa), and Type I collagenase from clostridium histolyticum were purchased from Sigma-Aldrich (St. Louis, MO, USA). 1-Ethyl-3-(3-dimethylaminopropyl) carbodiimide hydrochloride (EDC) and horseradish peroxidise (HRP, 304 units/mg) were purchased from Thermo Scientific (Rockford, IL, USA). Morpholinoethanesulfonic acid (MES) and N-hydroxysulfosuccinimide (NHS) were purchased from Acros Organics (New Jersey, USA). Hydrogen peroxide (H_2O_2) aqueous solution (35%, wt/wt) was purchased from BDH Chemicals (Westchester, PA, USA). Dialysis membrane (MWCO: 10 kD and 50 kD) were purchased from Spectrum® Laboratories (Dallas, TX, USA). Human umbilical vein endothelial cells (HUVECs) and endothelial cell growth media kits (EGM-2 BulletKit) were purchased from the Lonza Company (Allendale, NJ, USA). Recombinant mouse $VEGF_{164}$ and mouse VEGF Quantikine ELISA Kits were purchased from R&D Systems, Inc (Minneapolis, MN, USA). Fertile eggs (White Leghorns) were purchased from the Texas A&M University poultry science department (Bryan, TX, USA).

2.2 Synthesis of gelatin/tyramine/heparin (G/T/H) conjugates

As illustrated in Fig. 1, G/T/H was synthesized by two-step reactions. First, gelatin/tyramine (G/T) was synthesized as reported with minor modifications [26]. Briefly, gelatin type B (4 g) was dissolved in a 50 mM MES aqueous solution (200 ml) and was heated to 60°C. After dissolution of the gelatin, the solution was cooled to room temperature. EDC (1.5×10^{-3} mol/L) and NHS (0.75×10^{-3} mol/L) were added to the gelatin solution and allowed to activate for 15 mins. Tyramine (1 g) was added and the mixture was left to react for 12-24 hours at room temperature with gentle stirring. This modified polymer solution was dialyzed against deionized water, using standard regenerated cellulose dialysis tubing (MWCO: 10 kD) for at least 72 hours until an absorbance at 275 nm was undetectable in the filter solution using an UV spectrophotometer (NanoDrop 2000c, Thermo Scientific, DE, USA). The polymer solution was subsequently lyophilized. The content of tyramine in the G/T polymer was determined by measuring the absorbance of the polymer solution (1%, w/w) at 275 nm and calculated from a calibration curve obtained by measuring the absorbance of known percentages of tyramine in distilled water [26].

Next, heparin was incorporated onto the G/T conjugates by condensation of the carboxyl groups of the heparin and the amino groups of the gelatin via the EDC/NHS reaction system (Fig. 1). The lyophilized G/T (4g) was dissolved in aqueous solution (100 ml) containing 50 mM MES and 0.2 M NaCl, and then heated to 60°C. After dissolution of the G/T, the solution was cooled to room temperature. Heparin (1 g) was dissolved in another aqueous solution (100 ml) which had the same constituent (50 mM MES and 0.2 M NaCl). EDC (1.104 g) and NHS (0.264 g) were added to the heparin solution and allowed to activate for 15 mins. The G/T and activated heparin solution were mixed and allowed to react for 12-24 hours at room temperature under gentle stirring. The final product was dialyzed for at least 72 hours in 0.2 M NaCl solution before being transferred into deionized water using

standard regenerated cellulose dialysis tubing (MWCO: 50 kD). The purified G/T/H was lyophilized and stored in a desiccator for later use. The free amine assay of G/T and G/T/H is described in the following section (section 2.4).

2.3 Fourier transform infrared spectroscopy (FTIR) spectroscopy

FTIR spectra of gelatin, tyramine, heparin as well as their conjugates were recorded with an attenuated total reflectance (ATR) device on a Thermo Scientific Nicolet iSTM 10 FTIR spectrometer (Madison, Wisconsin, USA) at room temperature [34-36]. All spectra were calculated from 3600 to 500 cm^{-1} at 4 cm^{-1} spectral resolution and 64 scans.

2.4 Quantification of free amino groups in G/T and G/T/H

The residual number of free primary amino groups in gelatin after tyramine immobilization was determined with 2,4,6-trinitrobenzene sulfonic acid (TNBS, G-Biosciences, St. Louis, MO USA) [37]. Briefly, 500 μl of 0.1% (w/v) gelatin and G/T solution were added to a 250 μl working solution of 0.01% (w/v) TNBS in 0.1 M $NaHCO_3$ (pH 8.5) and mixed together. The mixture was incubated at 37°C for 2 hours. Subsequently, 250 μl 10% sodium dodecyl sulphate (SDS) and 125 μl 1N HCl were added to this solution to stop the reaction. The absorbance of the solution was measured at 335 nm. A calibration curve was obtained from the linear relationship between the absorbance and the known concentration of the L-Lysine. Each sample was repeated at least 3 times. The concentration of free amino groups (C) was calculated from the calibration curve and the number of amino groups per 1000 amino acids was obtained according to the following formula: $$\text{Free amino groups}=\frac{C\times MW(gelatin)}{0.1\%\times 146/2}$$ where MW(gelatin) is the molecular weight of gelatin, assuming of 10^5 g/mol for a gelatin molecular chain of 1000 amino acids [38], 146 g/mol is the molecular weight of L-Lysine, 2 is the number of free amino groups in L-Lysine, and C is the concentration of free amino groups.

2.5 Heparin content measurement

The amount of heparin incorporated to G/T was determined by a toluidine blue assay [39]. Briefly, 25 mg toluidine blue was dissolved in 500 ml 0.01 N hydrochloric acid (HCl) containing 0.2 wt% NaCl. Heparin solution (2 ml) with variable concentrations (0-25 μg/ml) was added to the 3 ml toluidine blue solution and incubated at 37°C for 2 hours. After incubation, 3 ml n-hexane was added to this solution, and the mixture was shaken well to extract the toluidine blue-heparin complex. The absorbance of the aqueous solution, which is caused by the unextracted toluidine blue, was measured by an UV spectrophotometer (NanoDrop 2000c, Thermo Scientific, DE, USA) at 631 nm. A calibration curve was obtained by the linear relationship between the absorbance and the concentration of the heparin. To determine the amount of heparin incorporated into the scaffold, 10 mg lyophilized G/T/H was dissolved in 50 ml deionized water, in which 2 ml of the G/T/H solution was added to the 3 ml toluidine blue solution and incubated at 37°C for 2 hours. Subsequently 3 ml n-hexane was added to extract the toluidine blue-heparin complex. Absorbance at 631 nm was measured and the content of heparin was calculated from the calibration curve as mentioned above.

2.6 Injectable G/T/H hydrogel preparation and gelation time measurement

G/T/H solution (190 μl) was prepared in 4 ml vials at room temperature. HRP powder was dissolved in 1×PBS solution at the concentration of 1 unit/5 μl for stock use. To form the gel, 5 μl diluted HRP were added into the G/T/H solution and thoroughly mixed, subsequently 5 μl diluted H_2O_2 solution was poured into each vial by gently shaking. The gelation time of the gelatin derivative was determined in 1×PBS solutions (pH 7.4) containing 1.5-5 wt% of G/T/H. The gelation time of the G/T/H hydrogels with different G/T/H, HRP and H_2O_2 concentrations was determined by the vial tilting method, and no flow within 1 min upon inverting the vial was considered as the gel state [40, 41]. Each experiment was repeated 3 times.

2.7 Mechanical property test

The specimens used for mechanical testing were prepared as followings: G/T/H solution (5 wt%, 990 μl) was dissolved in PBS and poured into a 5 ml syringe with the top barrel cut off (Fig. 6). Five microliter HRP (1 unit) was added to the solution and thoroughly mixed, 5 μl H_2O_2 solution with different concentrations were subsequently poured into the syringe by gentle shaking. After gelation, the cylindrical gels (12.5mm in diameter and 8.2mm in height) were obtained by pushing the plunger and positioned on a flat plate. Prior to the compression test, the initial position of the gel was defined as the starting point (distance 0 mm). The compressive modulus of the hydrogels was measured using a mechanical tester (TestResources, Shakopee, MN) at a compression rate of 10 mm/min [42].

2.8 *In vitro* enzymatic *degradation*

The G/T/H hydrogel samples were prepared by adding 250 μl G/T/H solutions into 4 ml plastic vials and forming the gel with the method described above. Subsequently the gels were immersed in 2 ml of PBS solution containing collagenase (10 unit/ml) and placed on an orbital shaker at 60 rpm at 37 °C for up to 12 hours. At different time points, the incubation medium was replaced and the remaining gel was weighed. The degradation ratios were expressed as the ratio of the remaining weight to the initial weight of the hydrogels. Different concentrations of G/T/H hydrogel and H_2O_2 were used. Three samples were prepared in each time point and each experiment was repeated twice.

2.9 Incorporation of VEGF into G/T/H and *in vitro* release kinetics

Two methods were used to load VEGF into the G/T and G/T/H hydrogels. In the first method, 100 μl 2.5% G/T and G/T/H hydrogels were prepared with the method mentioned above and then allowed to dry at room temperature. One microgram recombinant mouse $VEGF_{164}$ (R&D systems) was dissolved in 1×PBS containing 0.1% BSA (w/v) at the concentration of 100 μg/ml. Ten μl of VEGF solution was loaded with a micropipette onto the G/T or G/T/H hydrogels and allowed to be absorbed by the hydrogels at 4 °C for 18 hours. Subsequently, both of the hydrogels were soaked into 1 ml of release buffer [1×PBS containing 0.1% BSA (w/v)], after incubation at 37 °C for 30 minutes, all the supernatant was then aspirated and defined as unbound VEGF. In the second method, 1 μg recombinant mouse $VEGF_{164}$ was directly dissolved into 100 μl 2.5% G/T and G/T/H solutions, and then the gel was formed using the method mentioned above. For the VEGF release test, the G/T/

VEGF and G/T/H/VEGF hydrogels (100 μl) were immersed in 1 ml PBS buffer at 37°C. At a specific time point the release medium was collected and stored at -80 °C with 1 ml fresh medium replaced. At the last collection, the gels were soaked in 1 ml release buffer containing 30 unit/ml type I collagenase, and the VEGF in the final solution was defined as unreleased VEGF. After dissolution of the gel, all the samples were thawed and quantified using a Mouse VEGF Quantikine ELISA Kit (R&D systems). The initially bound VEGF was determined by adding all the released VEGF and unreleased VEGF together. Three samples were prepared in each time point and each experiment was repeated twice.

2.10 Bioactivity assay of released VEGF from G/T/H

The endothelial cell migration experiment was performed to examine the bioactivity of the released VEGF from the G/T/H [43, 44]. HUVECs were seeded into 12-multiwell plates at a density of 2×10^4 cells per well in EGM-2 BulletKit and incubated at 37 °C in 5% CO_2 humidified incubators for 6 hours to allow cell attachment. Then the medium was aspirated and replaced by EGM-2 basal medium without serum. After 12 hours of incubation, a line of HUVECs was scraped away using a universal blue pipette tip, and then the cells were washed twice with PBS and placed in a EGM-2 BulletKit without growth factors. Subsequently, 50 μl of released VEGF solution collected at 1 week, 2 weeks, 3 weeks, and 4 weeks was added to each well. In order to inhibit cell proliferation, 5 mM thymidine (Sigma, St Louis, MO, USA) was included during the incubation and the cells were cultured for 24 hours. They were fixed in 4% paraformaldehyde, stained with 5 μg/ml Hoechst 33342 to visualize the nuclei and photographed. Hoechst-positive nuclei that had moved into the scratched region were counted in five fields per well. Three samples were tested in each group and the means and standard error of the mean from triplicate wells were reported. Each experiment was repeated twice.

2.11 Chicken chorioallantoic membrane (CAM) assay

The *in vivo* bioactivity of VEGF released from the hydrogels was assessed by an open-shell chicken CAM assay[45]. Briefly, fertilized white leghorn chicken eggs (E0) were incubated at 37.8 °C for 3 days with 55-65% humidity, and the eggs were turned twice a day. On the third day (E3) of incubation, the eggs were moved out from the incubator. The embryos were positioned with a pencil under the egg candle lamp, and then sterilized with a 70% ethanol pad. The eggs were held horizontally with the pencil mark on top and opened into a 25×100 mm tissue culture petri dish, 200 μl gentamicin/amphotericin solution (Gibco, NY, USA) was added into the albumin. All of the steps in the processes were performed under the completely sterilized conditions in a Laminar Hood. The embryos in the petri dishes were then incubated at 37.8 °C with 70-90% humidity in aseptic conditions. On day 8 (E8), the VEGF (1 μg) loaded hydrogels (50 μl) were placed on the CAM away from the major exiting blood vessels. Pictures were taken from the region of the hydrogel location by means of the research stereomicroscopy using a digital camera at E13. Angiogenesis was assessed by counting the blood vessels surrounding the gels [46]. Three samples were prepared in each group and the each experiment was repeated twice.

2.12 *In vivo* animal experiment

The study was performed in compliance with the institutional regulations established and approved by the Animal Research Committee at the Texas A&M University Baylor College of Dentistry. Sixteen six-week-old male C57BL/6 inbred mice were purchased from Harlan Laboratories, Indianapolis, IN. Under anesthesia (xylazine:ketamine=5:1, v/v), each hydrogel (0.1 ml) loaded with 1 μg VEGF was subcutaneously injected into the dorsal side of the mice using a 29-gauge needle. At the end of two weeks, the mice were sacrificed, and the subcutaneous tissues containing the gels were excised, fixed in 4% paraformaldehyde solution, paraffin embedded, sectioned, and stained with hematoxylin-eosin (H&E) and anti-α smooth muscle actin (aSMA) antibody (abcam, Cambridge, MA). The blood vessel density and area in 5 different fields (200× magnification), randomly selected from captured images of 3 immunohistochemical staining slides from each animal, was determined using Image Pro Plus software (version 6.0, Media Cybernatics, USA).

2.13 Statistical analysis

Quantitative results are presented as mean ± standard deviation (S.D), unless stated otherwise. Statistical significance was determined using a two-sided Student's t-test; a value of $P<0.05$ was considered significant.

3. Results

3.1 Synthesis and characterization of the G/T/H

As illustrated in Fig. 1, a two-step reaction process was developed to synthesize G/T/H. In the first step, tyramine was conjugated onto the gelatin chains by crosslinking the carboxyl groups of the gelatin with the amino groups of the tyramine. The phenyl group of the tyramine has strong absorption at 275 nm [26] and was selected to detect the tyramine in the G/T. Compared to the gelatin alone, the absorbance of G/T at 275 nm significantly increased; indicating that tyramine was successfully introduced onto the gelatin chains (Fig. 2a). The amount of tyramine incorporated onto the gelatin chains was controlled by the concentration of EDC in the reaction mixture. As shown in Fig. 2b, increasing the EDC concentration led to a higher amount of tyramine in the G/T. Meanwhile, the free amino groups in the gelatin chains of the G/T was 20.8±1.6/(1000 amino acids), which was similar to the value of 23.2±1.1/(1000 amino acids) in the original gelatin ($P>0.05$), indicating that most of the free amino groups in the gelatin chains of the G/T remain intact.

Next, heparin was introduced into the G/T by a coupling reaction of the carboxyl groups of heparin with the amino groups of gelatin (Fig. 1b); the FTIR spectra of the resultant G/T/H are shown in Fig. 3. The characteristic absorption peaks of G/T/H at 1222 cm-1 (dashed line A) and 1145 cm-1 (dashed line B) were assigned to the asymmetric and symmetric stretching vibrations of the O=S=O group in the heparin, respectively [47, 48]. In addition, the band of G/T/H at 1024 cm-1 (dashed line C) was attributed to the $-SO_3$ group of the heparin [49]. These results confirmed that heparin was coupled into the G/T/H. Increasing the concentration of heparin during the coupling reaction led to an increased amount of heparin in the G/T/H. As shown in Fig. 4, the amount of immobilized heparin in the G/T/H increased from 1.13±0.21% (wt/wt) to 7.71±0.87% (wt/wt) when the heparin concentration

in the reactants increased from 0.05 g/ml to 0.5 g/ml. In addition, the value of the free amino groups in the G/T/H was 10.3±1.5/(1000 amino acids), which was 50% less than that in the G/T [20.8±1.6/(1000 amino acids)], confirming the success of coupling the heparin to the G/T.

3.2 Formation of G/T/H hydrogels and gelation time measurement

The injectable G/T/H hydrogel was rapidly formed by an enzymatically crosslinked reaction using HRP and H_2O_2 (Fig. 1c and the video in the Supporting Information). The gelation time ranged from a few seconds to several minutes and was controlled by varying the concentration of H_2O_2, HRP and G/T/H (Fig. 5). Generally, the gelation time increased with the H_2O_2 concentration under the same G/T/H and HRP concentration (Fig. 5a). Under the same G/T/H and H_2O_2 conditions, a higher HRP concentration led to a shorter time to form a gel (Fig. 5a). The gelation time also decreased with a higher G/T/H concentration (Fig. 5b).

3.3 Control of the mechanical strength of G/T/H hydrogels

The mechanical strength of the G/T/H hydrogels was readily controlled by varying the concentration of H_2O_2. As shown in Fig. 6, the storage modulus of the G/T/H increased with the concentration of H_2O_2 and reached the highest value when the H_2O_2 concentration was 5 mM. Further increasing the concentration of H_2O_2 led to the decrease of the mechanical strength.

3.4 *In vitro* degradation of the G/T/H hydrogels

The *in vitro* enzymatic degradation of G/T/H was performed in PBS solution containing collagenase (10 unit/ml) using a series of samples with different concentrations of G/T/H and H_2O_2 (Fig. 7). Overall, low-concentration gels degraded faster than the high-concentration gels. For example, the weight of the 1.5 wt% G/T/H gel decreased by 65% after 3 hours of incubation, and the gel was completely dissolved within 7 hours. However, more than 30% of its initial weight remained in the 5 wt% G/T/H gel after 9-hour incubation (Fig. 7a). As the H_2O_2 increased from a low concentration to 5 mM, the degradation rate of the G/T/H decreased, and further increase of the H_2O_2 concentration led to faster G/T/H degradation (Fig. 7b). This trend was consistent with the mechanical property assay shown in Fig. 6.

3.5 *In vitro* release of VEGF from the G/T/H hydrogels

Two approaches were utilized to incorporate VEGF into the G/T and the G/T/H hydrogels and were analyzed using an ELISA assay. In the first method in which VEGF was physically adsorbed into the hydrogel after gel formation, a high burst release was observed in the G/T hydrogel and 82.1% of the VEGF was released on the first day, while only 23.7% of the VEGF in the G/T/H group was released during the first 24 h (Fig 8a). After 7 days, 94.3% of the VEGF was released in the G/T group, while 65.6% of the VEGF was still retained in the G/T/H hydrogel (Fig. 8a). Similar results were observed in the second approach in which VEGF was dissolved in the G/T/H solution before the gel formation (Fig. 8b). The G/T group had a higher burst release (34.6%) than the G/T/H (25.5%) on the first

day. Over 54.1% of VEGF was released from the G/T, while only 36.0% of VEGF was released from the G/T/H after 21 days. These results indicated that the loading method had a significant effect on VEGF release and the G/T/H hydrogel was more efficient at binding the VEGF and controlling its release from the gel compared to the G/T. For the following *in vitro* and *in vivo* experiments, we chose the second method to load VEGF into the G/T/H and tested the bioactivity and new blood vessel formation of the released VEGF from the G/T/H hydrogel.

3.6 *In vitro* bioactivity assay of the released VEGF from the G/T/H hydrogels

Human umbilical vein endothelial cells (HUVECs) were used in a cell scratch assay to evaluate the bioactivity of the released VEGF from the G/T/H hydrogel. VEGF solution (containing 10 ng VEGF) released from the G/T/H hydrogel at 1, 2, 3, and 4 weeks was collected and used to treat the HUVECs and compared to the control and the VEGF standard (10 ng) groups. As shown in Fig. 9, more cells migrated to the scratched region in the 1w experimental group (Fig. 9b) than in the control group (Fig.9a) after culturing for 24 h. Similar results were observed for the other three experimental groups. The quantitative analyses indicated that the cell number in the scratched region of the 1w, 2w, 3w, and 4w groups was 85±21, 90±7, 110±30 and 83±7, respectively, which was significantly higher than the control group (38±6) ($P< 0.05$) (Fig. 9c). The average migration distance of the HUVECs in the control group was 77.4±3.8 μm, which was significantly shorter than the distances in the experimental groups (129.4±4.4, 133.6±4.0, 141.9±4.3 and 140.0±4.7 μm, for 1w, 2w, 3w and 4w groups, respectively) (Fig. 9d). In addition, both the cell number in the scratched region and the average cell migration distance in the experimental groups (1w, 2w, 3w, and 4w) were similar to those in the VEGF standard group, indicating that the released VEGF (up to 4 weeks) from the G/T/H gels retained its high bioactivity.

3.7 *In vivo* CAM assay

The capacity of the VEGF-loaded hydrogel to induce angiogenesis was examined by implanting gels on the embryonic day 8 (E8) CAM, which was the best time for the treatment of the vessel network (Fig. 10a) [50]. After 5 days' incubation, the control group showed a normal CAM vessel network, and the growth process of the blood vessels was random (Fig. 10d). In contrast, more blood vessels grew radially toward the VEGF-containing hydrogels than the control (Fig 10b&10c). The quantitative analysis confirmed that the numbers of blood vessels surrounding the VEGF-containing G/T (30±6) and G/T/H (42±4) gels were significantly higher than the control group (18±3, $P<0.05$) (Fig. 10e). Additionally, the number of new blood vessels in the G/T/H+VEGF group also showed a significant increase compared to the G/T+VEGF group ($P<0.05$).

3.8 *In vivo* angiogenesis

Fig. 11 shows the gross view of the implanted hydrogels after being subcutaneously injected into the dorsal side of mice for 2 weeks. The color of the G/T hydrogel (Fig. 11a) was pale and transparent, and very few blood vessels were found on the surface or inside the G/T hydrogel. For the G/T/H specimens, some blood vessels were observed surrounding the gel and a few of them extended inside the hydrogel (Fig. 11b). The color of the VEGF-loaded

G/T hydrogel was brownish-red (Fig. 11c), and many blood vessels had formed on the surface. In contrast, the VEGF-loaded G/T/H group showed a number of new blood vessels formed both on the surface and inside the gel, leading to a red appearance of the VEGF-loaded G/T/H (Fig. 11d).

In the H&E staining, the G/T group showed a minor cell infiltration along the edge of the G/T gel, whereas the other three groups (G/T/H, VEGF-loaded G/T, and VEGF-loaded G/T/H) all displayed a moderate cell infiltration (Fig. 12). Few blood vessels were found at the margin of the G/T hydrogel, while more blood vessels were detected in the other three groups (Fig. 12, arrowheads). Furthermore, more blood vessels were observed in the interior area of the VEGF-loaded G/T/H hydrogel than the VEGF-loaded G/T group. These results were further confirmed by immunohistochemical staining of α-SMA in the hydrogel constructs (Fig. 13). The quantitative analyses also showed that the average blood vessel numbers were 14.5, 52.3, 87.2 and 182.7 per mm^2 for the G/T, G/T/H, VEGF-loaded G/T and VEGF-loaded G/T/H, respectively (Fig. 14a). And the average blood vessel area in the G/T, G/T/H, VEGF-loaded G/T and VEGF-loaded G/T/H groups were 0.66%, 1.27%, 2.1% and 5.95%, respectively (Fig. 14b). Taken together, these results showed that the VEGF-loaded G/T/H had significantly higher average blood vessel number and area than the other three groups.

4 Discussion

Soft tissue regeneration has been explored for over two decades; however, development of proper scaffolding biomaterials to form adipose tissues with high-dimensional stability has not been achieved yet. One promising approach to solve this problem is fast vascularization of the bioengineered soft tissue. Meanwhile, since most of the soft tissue is regenerated for the aesthetic and cosmetic purposes, delivery scaffolding biomaterials in a minimal invasive manner is highly desired. Consequently, controlled injectability of the scaffolding biomaterial is an important parameter. In this study, we designed and synthesized a new type of gelatin-derivative hydrogel that has well-controlled injectability and possesses sustained VEGF delivery to induce and accelerate angiogenesis within a short period of time.

We developed a three-step approach to synthesizing the gelatin-derivative hydrogels. First, we incorporated tyramine onto the main chain of the gelatin to provide crosslinking points for the gelatin derivative. In order to protect the primary amino groups in gelatin chains, which will be used to react with heparin, we added an excess amount of tyramine [molar ratio: -NH_2(tyramine)/-COOH(gelatin) >10] during the coupling reaction. Trinitrobenzene sulfonic acid (TNBS) reacts specifically with the primary amino group and was used to determine free primary amino groups in gelatin chains [51]. The quantitative analysis confirmed that number of the free amino groups in the gelatin chains of the G/T was close to that in the original gelatin chains, similar to the result reported by Kale et al. [52]. Next, we introduced heparin to the gelatin derivative (G/T) to form G/T/H, which presented binding domains for VEGF. The decrease of the free amino groups in the gelatin chains of G/T demonstrated the success of coupling G/T with heparin. Finally, when the VEGF was loaded into the G/T/H and mixed with the HRP/H_2O_2, it formed an injectable hydrogel. We added tyramine to the gelatin because it formed a hydrogel through HRP/H_2O_2-activated

crosslinking reaction under physiological conditions. During the crosslinking reaction, the phenol moieties of the G/T/H were conjugated with each other via either the carbon-carbon bond at the ortho position or the carbon-oxygen bond between the carbon at the ortho position and the phenoxy oxygen [33]. Another advantage of this hydrogel formation system is the high viability (≥95%) of the cells encapsulated in the hydrogel [26]. In addition, compared to other crosslinking systems whose gelation process is time-consuming (e.g. using glutaraldehyde and carbodiimides requires several hours), the use of H_2O_2 for *in situ* gelation of the gelatin derivatives requires only a few seconds to minutes (see the video in the Supporting Information), which gives it a significant advantage for biomedical application. As shown in Fig. 5, the gelation time was controlled by the concentration of HRP, H_2O_2 and G/T/H. Increasing the concentration of HRP and G/T/H led to a shorter gelation time. Under the same concentration of HRP and G/T/H, increasing the concentration of H_2O_2 resulted in a longer gelation time, which was caused by the fact that the excess amount of H_2O_2 led to the decreased activity of HRP [33].

The mechanical strength of the G/T/H increased with the crosslinking density of the hydrogel, which was controlled in several ways. The first method involved controlling the number of pyrrole units linked to the G/T/H, which was achieved by altering the amount of the crosslinking agent (EDC/NHS). Generally, the extent of pyrrole units increased with the amount of EDC/NHS in the G/T hydrogels [26]. In our G/T/H hydrogel system, we modified the reaction conditions and fabricated G/T/H hydrogels with reasonably high mechanical strength at the G/T/H concentration of 2.5% wt/v. Another way to control the extent of crosslinking between the pyrrole units is to vary the concentration of HRP, H_2O_2 and G/T/H. A higher G/T/H concentration led to a higher modulus of the G/T/H hydrogels. Under the same concentrations of G/T/H and HRP, the mechanical strength of the G/T/H hydrogels increased when the concentration of H_2O_2 increased from 1 mM to 5 mM (Fig. 6). Further increasing the amount of H_2O_2 led to a lower mechanical strength of the G/T/H hydrogels. Similar results were observed in the G/T hydrogel system, and were attributed to the deactivation of HRP by a high concentration of H_2O_2 [26]. However, the high concentration of H_2O_2 may also trigger the degradation of the gelatin matrix, leading to the decrease of the mechanical strength of the G/T/H hydrogels. This result indicated that the mechanical properties of the G/T/H hydrogels could be readily modulated by the H_2O_2 concentration. Considering the toxicity of H_2O_2 to the cells, we selected a low concentration of H_2O_2 (1 mM) in our G/T/H hydrogel for the *in vitro* and *in vivo* studies.

VEGF is an angiogenic factor consisting of four alternatively spliced forms, three of which interact with heparin [53, 54]. The binding of VEGF to its receptors is dependent on cell surface-associated heparin-like molecules [54]. Heparin in the ECM serves as a reservoir for VEGF and promotes its long-term bioavailability. It has been reported that gelatin/heparin conjugate was able to selectively immobilize VEGF, even in the presence of albumin, with an efficiency of 54.2% [55]. Therefore, we introduced heparin into the G/T/H hydrogel via a carbodiimide-mediated condensation reaction between the carboxyl groups of heparin and the amino groups of gelatin. As shown in Fig 4, the heparin amount of the G/T/H was controlled by the concentration of heparin in the reaction mixture. As heparin is also an anti-

coagulant factor, a high amount of heparin may cause haemorrhage at the implant site. In our G/T/H conjugate, the amount of heparin ranged between 1.13-7.71%.

The degradation of the G/T/H hydrogel was readily controlled by the G/T/H and H_2O_2 concentrations (Fig. 7). It should be pointed out that in order to accelerate the *in vitro* degradation process, a relatively high concentration of collagenase (10 unit/ml) was added to the degradation medium. When placed in PBS only, the G/T/H hydrogel was very stable and degraded much more slowly than in the PBS with collagenase. To truly reflect the degradation profile of the G/T/H in contact with body fluid, an *in vivo* degradation measurement is needed in future studies.

We developed two methods to load VEGF into G/T/H and examine its release profiles from the hydrogel (Fig. 8). In both methods, both G/T/H and G/T revealed a biphasic release profile, that is, there was an initial burst of VEGF followed by a gradual and sustained release. However, the burst release of VEGF in the G/T/H group was significantly lower than in the G/T. Furthermore, regardless that the VEGF was physically adsorbed onto the G/T/H after gelation (method 1) or directly added in the G/T/H before gelation (method 2), the burst release of VEGF from the G/T/H had similar values (23.7% *vs*. 25.5%). These results confirmed that heparin had high binding affinity with VEGF and the incorporation of heparin into the hydrogel effectively controlled the release profile of VEGF from the G/T/H.

The bioactivity of the released VEGF from the hydrogels is another important question to address. We first utilized the released VEGF to treat HUVECs and examine their migration. Fig. 9 shows that even after a long incubation (up to 4 weeks), the released VEGF from the G/T/H still retained its bioactivity promoting the migration of HUVEC, as reflected by the cell number and average migration distance. Subsequently, *in vivo* CAM assay was carried out to verify the possibility of using this VEGF-loaded hydrogel for growing capillary networks. As shown in Fig. 10e, a significantly higher number of blood vessels were found in the VEGF-loaded G/T/H hydrogel than in other groups. Since the *in vivo* CAM model of angiogenesis is suitable only for short-term experiments, we further used a mouse model to verify the angiogenic response for a longer time. After subcutaneous injection in mice for 2 weeks, all gels were formed *in situ* and encapsulated in dense connective tissue, which further confirmed the good injectability and compatibility of the G/T/H. The gross view and histological observation revealed that both the heparin-modified hydrogels and VEGF-loaded G/T hydrogel demonstrated a better performance on cell infiltration, blood vessel density and blood vessel area than the G/T control ($p<0.05$). Furthermore, VEGF-loaded G/T/H hydrogel had the highest blood vessel density and the deepest infiltration of the blood vessels compared to other groups ($p<0.05$). In addition, the G/T/H hydrogel without VEGF also had a higher blood vessel density and infiltration of blood vessels than the G/T hydrogel ($p<0.05$), indicating that the incorporation of heparin alone into G/T might also have the ability to induce angiogenesis to a certain degree. We believe that the highest vascularization of the VEGF-loaded G/T/H is attributed to the following two major factors. First, the binding of VEGF to heparin protects the VEGF from denaturation and proteolytic degradation [56]. Second, a heparin-modified hydrogel provides a more sustained release of the VEGF over a long time period. In our future study, we will integrate adipose derived

stem cells into the G/T/H hydrogel and test the long-term viability and stability of the regenerated adipose tissue.

5 Conclusion

This study presents a tunable injectable biomimetic hydrogel for rapid angiogenesis. The properties of the injectable hydrogel, such as gelation time, mechanical strength and degradation rate, were controlled by the concentrations of HRP, H_2O_2, and G/T/H. The *in vitro* and *in vivo* data indicated that the G/T/H hydrogel not only provided a controlled release of VEGF from the hydrogel, but also retained the bioactivity of the VEGF for a long time. Furthermore, even without the incorporation of VEGF into the gel, the G/T/H itself had the ability to induce angiogenesis to a certain degree. G/T/H hydrogel, therefore, has great potential as an injectable scaffold for soft tissue regeneration and a carrier for controlled drug delivery.

Supplementary Material

Refer to Web version on PubMed Central for supplementary material.

Acknowledgments

This study was supported by NIH/NIDCR 1R03DE22838-01A1, Texas A&M-Weizmann Collaborative Program, and Texas A&M-NSFC Collaborative Program to X.L, and the State Scholarship Fund of China (No. 201207610010) to Z.L. We would like to thank Jeanne Santa Cruz for her assistance with the editing of this article.

References

1. Patrick CW Jr. Tissue engineering strategies for adipose tissue repair. Anat Rec. 2001; 263:361–6. [PubMed: 11500812]
2. Choi JH, Gimble JM, Lee K, Marra KG, Rubin JP, Yoo JJ, et al. Adipose tissue engineering for soft tissue regeneration. Tissue Eng Part B. 2010; 16:413–26.
3. http://www.plasticsurgery.org/news/press-release-archives/2013/14-million-cosmetic-plastic-surgery-procedures-performed-in-2012.html, 14.6 Million Cosmetic Plastic Surgery Procedures Performed in 2012, Retrieved on 3/28/2014.
4. Wang W, Cao B, Cui L, Cai J, Yin J. Adipose tissue engineering with human adipose tissue-derived adult stem cells and a novel porous scaffold. J Biomed Mater Res B Appl Biomater. 2013; 101:68–75. [PubMed: 23090921]
5. Duranti F, Salti G, Bovani B, Calandra M, Rosati ML. Injectable hyaluronic acid gel for soft tissue augmentation - A clinical and histological study. Dermatol Surg. 1998; 24:1317–25. [PubMed: 9865196]
6. Eppley BL, Dadvand B. Injectable soft-tissue fillers: clinical overview. Plast Reconstr Surg. 2006; 118:98E–106E.
7. Lemperle G, Morhenn V, Charrier U. Human histology and persistence of various injectable filler substances for soft tissue augmentation. Aesthet Plast Surg. 2003; 27:354–66.
8. Christensen L, Breiting V, Janssen M, Vuust J, Hogdall E. Adverse reactions to injectable soft tissue permanent fillers. Aesthet Plast Surg. 2005; 29:34–48.
9. Lowe NJ, Maxwell CA, Patnaik R. Adverse reactions to dermal fillers: review. Dermatol Surg. 2005; 31:1616–25. [PubMed: 16416647]
10. Alhadlaq A, Tang M, Mao JJ. Engineered adipose tissue from human mesenchymal stem cells maintains predefined shape and dimension: implications in soft tissue augmentation and reconstruction. Tissue Eng. 2005; 11:556–66. [PubMed: 15869434]

11. Casadei A, Epis R, Ferroni L, Tocco I, Gardin C, Bressan E, et al. Adipose tissue regeneration: a state of the art. J Biomed Biotechnol. 2012
12. Lendeckel S, Jodicke A, Christophis P, Heidinger K, Wolff J, Fraser JK, et al. Autologous stem cells (adipose) and fibrin glue used to treat widespread traumatic calvarial defects: case report. J Cranio Maxill Surg. 2004; 32:370–3.
13. Torio-Padron N, Baerlecken N, Momeni A, Stark GB, Borges J. Engineering of adipose tissue by injection of human preadipocytes in fibrin. Aesthet Plast Surg. 2007; 31:285–93.
14. Vermette M, Trottier V, Menard V, Saint-Pierre L, Roy A, Fradette J. Production of a new tissue-engineered adipose substitute from human adipose-derived stromal cells. Biomaterials. 2007; 28:2850–60. [PubMed: 17374391]
15. Patel ZS, Yamamoto M, Ueda H, Tabata Y, Mikos AG. Biodegradable gelatin microparticles as delivery systems for the controlled release of bone morphogenetic protein-2. Acta Biomater. 2008; 4:1126–38. [PubMed: 18474452]
16. Sarkanen JR, Kaila V, Mannerstrom B, Raty S, Kuokkanen H, Miettinen S, et al. Human adipose tissue extract induces angiogenesis and adipogenesis in vitro. Tissue Eng Part A. 2012; 18:17–25. [PubMed: 21902602]
17. Vashi AV, Abberton KM, Thomas GP, Morrison WA, O'Connor AJ, Cooper-White JJ, et al. Adipose tissue engineering based on the controlled release of fibroblast growth factor-2 in a collagen matrix. Tissue Eng. 2006; 12:3035–43. [PubMed: 17518619]
18. Kang JH, Gimble JM, Kaplan DL. In vitro 3D model for human vascularized adipose tissue. Tissue Eng Part A. 2009; 15:2227–36. [PubMed: 19207036]
19. Sarkanen JR, Ruusuvuori P, Kuokkanen H, Paavonen T, Ylikomi T. Bioactive acellular implant induces angiogenesis and adipogenesis and sustained soft tissue restoration in vivo. Tissue Eng Part A. 2012; 18:2568–80. [PubMed: 22738319]
20. Tabata Y, Ikada Y. Protein release from gelatin matrices. Adv Drug Deliver Rev. 1998; 31:287–301.
21. Liu X, Smith LA, Hu J, Ma PX. Biomimetic nanofibrous gelatin/apatite composite scaffolds for bone tissue engineering. Biomaterials. 2009; 30:2252–8. [PubMed: 19152974]
22. Liu XH, Ma PX. Phase separation, pore structure, and properties of nanofibrous gelatin scaffolds. Biomaterials. 2009; 30:4094–103. [PubMed: 19481080]
23. Sun Y, Jiang Y, Liu QJ, Gao T, Feng JQ, Dechow P, et al. Biomimetic engineering of nanofibrous gelatin scaffolds with noncollagenous proteins for enhanced bone regeneration. Tissue Eng Part A. 2013; 19:1754–63. [PubMed: 23469769]
24. Mazaki T, Shiozaki Y, Yamane K, Yoshida A, Nakamura M, Yoshida Y, et al. A novel, visible light-induced, rapidly cross-linkable gelatin scaffold for osteochondral tissue engineering. Sci Rep. 2014; 4:4457. [PubMed: 24662725]
25. Dash R, Foston M, Ragauskas AJ. Improving the mechanical and thermal properties of gelatin hydrogels cross-linked by cellulose nanowhiskers. Carbohydr Polym. 2013; 91:638–45. [PubMed: 23121958]
26. Sakai S, Hirose K, Taguchi K, Ogushi Y, Kawakami K. An injectable, in situ enzymatically gellable, gelatin derivative for drug delivery and tissue engineering. Biomaterials. 2009; 30:3371–7. [PubMed: 19345991]
27. Amini AA, Nair LS. Enzymatically cross-linked injectable gelatin gel as osteoblast delivery vehicle. J Bioact Compat Pol. 2012; 27:342–55.
28. Gerber HP, Hillan KJ, Ryan AM, Kowalski J, Keller GA, Rangell L, et al. VEGF is required for growth and survival in neonatal mice. Development. 1999; 126:1149–59. [PubMed: 10021335]
29. Carmeliet P, Jain RK. Molecular mechanisms and clinical applications of angiogenesis. Nature. 2011; 473:298–307. [PubMed: 21593862]
30. Singh S, Wu BM, Dunn JCY. The enhancement of VEGF-mediated angiogenesis by polycaprolactone scaffolds with surface cross-linked heparin. Biomaterials. 2011; 32:2059–69. [PubMed: 21147501]
31. Ono K, Hattori H, Takeshita S, Kurita A, Ishihara M. Structural features in heparin that interact with VEGF(165) and modulate its biological activity. Glycobiology. 1999; 9:705–11. [PubMed: 10362840]

32. Pike DB, Cai SS, Pomraning KR, Firpo MA, Fisher RJ, Shu XZ, et al. Heparin-regulated release of growth factors in vitro and angiogenic response in vivo to implanted hyaluronan hydrogels containing VEGF and bFGF. Biomaterials. 2006; 27:5242–51. [PubMed: 16806456]
33. Park KM, Ko KS, Joung YK, Shin H, Park KD. In situ cross-linkable gelatin-poly(ethylene glycol)-tyramine hydrogel via enzyme-mediated reaction for tissue regenerative medicine. J Mater Chem. 2011; 21:13180–7.
34. Liu XH, Smith L, Wei GB, Won YJ, Ma PX. Surface engineering of nano-fibrous poly(L-Lactic Acid) scaffolds via self-assembly technique for bone tissue engineering. J Biomed Nanotech. 2005; 1:54–60.
35. Liu, XH.; Won, YJ.; Ma, PX. Surface engineering of nano-fibrous biodegradable poly(L-lactic acid) scaffolds for tissue engineering. In: Aizenberg, J.; Landis, WJ.; Orme, C.; Wang, R., editors. Biological and Bioinspired Materials and Devices. Warrendale: Materials Research Society; 2004. p. 243-8.
36. Liu XH, Won YJ, Ma PX. Surface modification of interconnected porous scaffolds. J Biomed Mater Res Part A. 2005; 74A:84–91.
37. Steffens GC, Yao C, Prevel P, Markowicz M, Schenck P, Noah EM, et al. Modulation of angiogenic potential of collagen matrices by covalent incorporation of heparin and loading with vascular endothelial growth factor. Tissue Eng. 2004; 10:1502–9. [PubMed: 15588409]
38. Kuijpers AJ, Engbers GH, Krijgsveld J, Zaat SA, Dankert J, Feijen J. Cross-linking and characterisation of gelatin matrices for biomedical applications. J Biomater Sci Polym Ed. 2000; 11:225–43. [PubMed: 10841277]
39. Gumusderelioglu M, Aday S. Heparin-functionalized chitosan scaffolds for bone tissue engineering. Carbohydr Res. 2011; 346:606–13. [PubMed: 21333274]
40. Park KM, Shin YM, Joung YK, Shin H, Park KD. In situ forming hydrogels based on tyramine conjugated 4-Arm-PPO-PEO via enzymatic oxidative reaction. Biomacromolecules. 2010; 11:706–12. [PubMed: 20121075]
41. Jin R, Moreira Teixeira LS, Dijkstra PJ, Karperien M, van Blitterswijk CA, Zhong ZY, et al. Injectable chitosan-based hydrogels for cartilage tissue engineering. Biomaterials. 2009; 30:2544–51. [PubMed: 19176242]
42. Qu TJ, Liu XH. Nano-structured gelatin/bioactive glass hybrid scaffolds for the enhancement of odontogenic differentiation of human dental pulp stem cells. J Mater Chem B. 2013; 1:4764–72.
43. Matsumoto T, Bohman S, Dixelius J, Berge T, Dimberg A, Magnusson P, et al. VEGF receptor-2 Y951 signaling and a role for the adapter molecule TSAd in tumor angiogenesis. EMBO J. 2005; 24:2342–53. [PubMed: 15962004]
44. Bhattacharya R, Kwon J, Li X, Wang E, Patra S, Bida JP, et al. Distinct role of PLCbeta3 in VEGF-mediated directional migration and vascular sprouting. J Cell Sci. 2009; 122:1025–34. [PubMed: 19295129]
45. Singh S, Wu BM, Dunn JC. Delivery of VEGF using collagen-coated polycaprolactone scaffolds stimulates angiogenesis. J Biomed Mater Res A. 2012; 100:720–7. [PubMed: 22213643]
46. Bronckaers A, Hilkens P, Fanton Y, Struys T, Gervois P, Politis C, et al. Angiogenic properties of human dental pulp stem cells. PLoS One. 2013; 8:e71104. [PubMed: 23951091]
47. Martins AF, Pereira AGB, Fajardo AR, Rubira AF, Muniz EC. Characterization of polyelectrolytes complexes based on N,N,N-trimethyl chitosan/heparin prepared at different pH conditions. Carbohydr Polym. 2011; 86:1266–72.
48. Gao AL, Liu F, Xue LX. Preparation and evaluation of heparin-immobilized poly (lactic acid) (PLA) membrane for hemodialysis. J Membr Sci. 2014; 452:390–9.
49. Wang JL, Hu W, Liu Q, Zhang SM. Dual-functional composite with anticoagulant and antibacterial properties based on heparinized silk fibroin and chitosan. Colloid Surf B. 2011; 85:241–7.
50. Namvar F, Mohamad R, Baharara J, Zafar-Balanejad S, Fargahi F, Rahman HS. Antioxidant, antiproliferative, and antiangiogenesis effects of polyphenol-rich seaweed (Sargassum muticum). Biomed Res Int. 2013; 2013:604787. [PubMed: 24078922]

51. Bubnis WA, Ofner CM. The determination of epsilon-amino groups in soluble and poorly soluble proteeinaceous by a spectrophotometric method using trinitrobenzenesulfonic acid. Anal Biochem. 1992; 207:129–33. [PubMed: 1489085]

52. Kale R, Bajaj A. Ultraviolet spectrophotometric method for determination of gelatin crosslinking in the presence of amino groups. J Young Pharm. 2010; 2:90–4. [PubMed: 21331199]

53. Capila I, Linhardt RJ. Heparin - protein interactions. Angew Chem Int Ed. 2002; 41:391–412.

54. Gitaygoren H, Soker S, Vlodavsky I, Neufeld G. The binding of vascular endothelial growth factor to its receptors is dependent on cell surface-associated heparin-like molecules. J Biol Chem. 1992; 267:6093–8. [PubMed: 1556117]

55. Nakamura S, Kubo T, Ijima H. Heparin-conjugated gelatin as a growth factor immobilization scaffold. J Biosci Bioeng. 2013; 115:562–7. [PubMed: 23273911]

56. Oliviero O, Ventre M, Netti PA. Functional porous hydrogels to study angiogenesis under the effect of controlled release of vascular endothelial growth factor. Acta Biomater. 2012; 8:3294–301. [PubMed: 22641106]

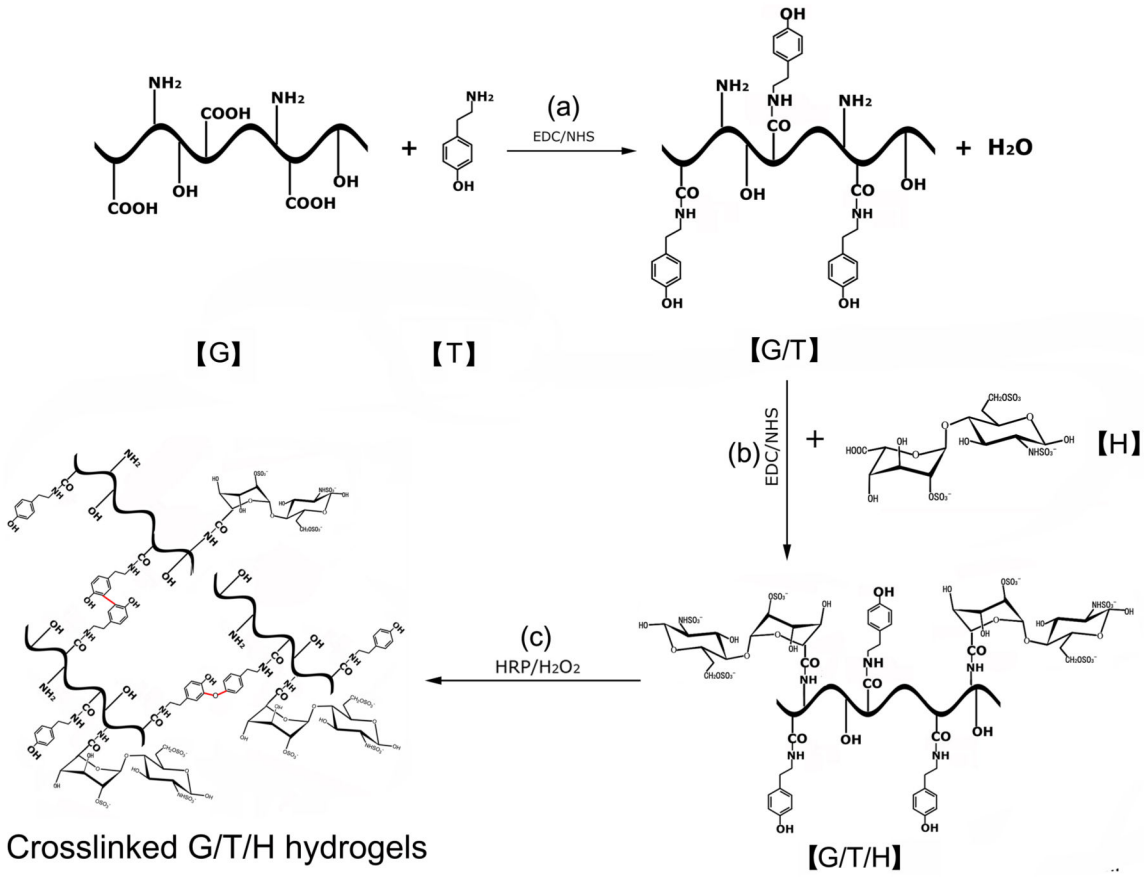

Fig 1.

Illustration of the synthesis of gelatin/tyramine/heparin (G/T/H) hydrogels. (**a**) Synthesis of gelatin/tyramine (G/T) by the coupling of the -COOH in the gelatin chains with the $-NH_2$ in the tyramine. (**b**) Synthesis of G/T/H conjugates by the condensation of the -COOH in the heparin and the $-NH_2$ in the gelatin. (**c**) Addition of HRP and H_2O_2 to form injectable G/T/H hydrogels.

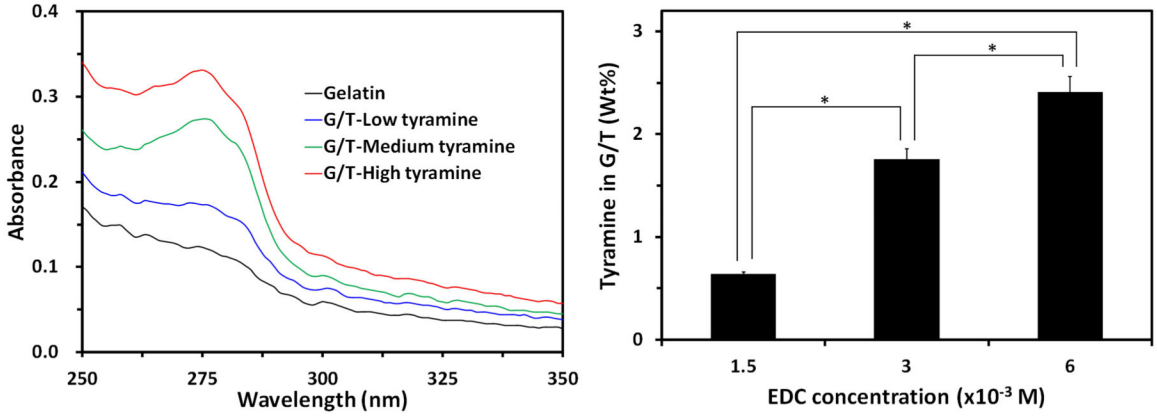

Fig 2.

Characterization of G/T. (**a**) UV-Vis absorbance spectra of the G/T with different contents of tyramine. The concentration of the G/T was at 1% wt/wt. (**b**) Tyramine content in the G/T using different concentration of EDC. The ratio of gelatin to tyramine was 4/1 (wt/wt) in the reagent solution. * denotes $p<0.05$.

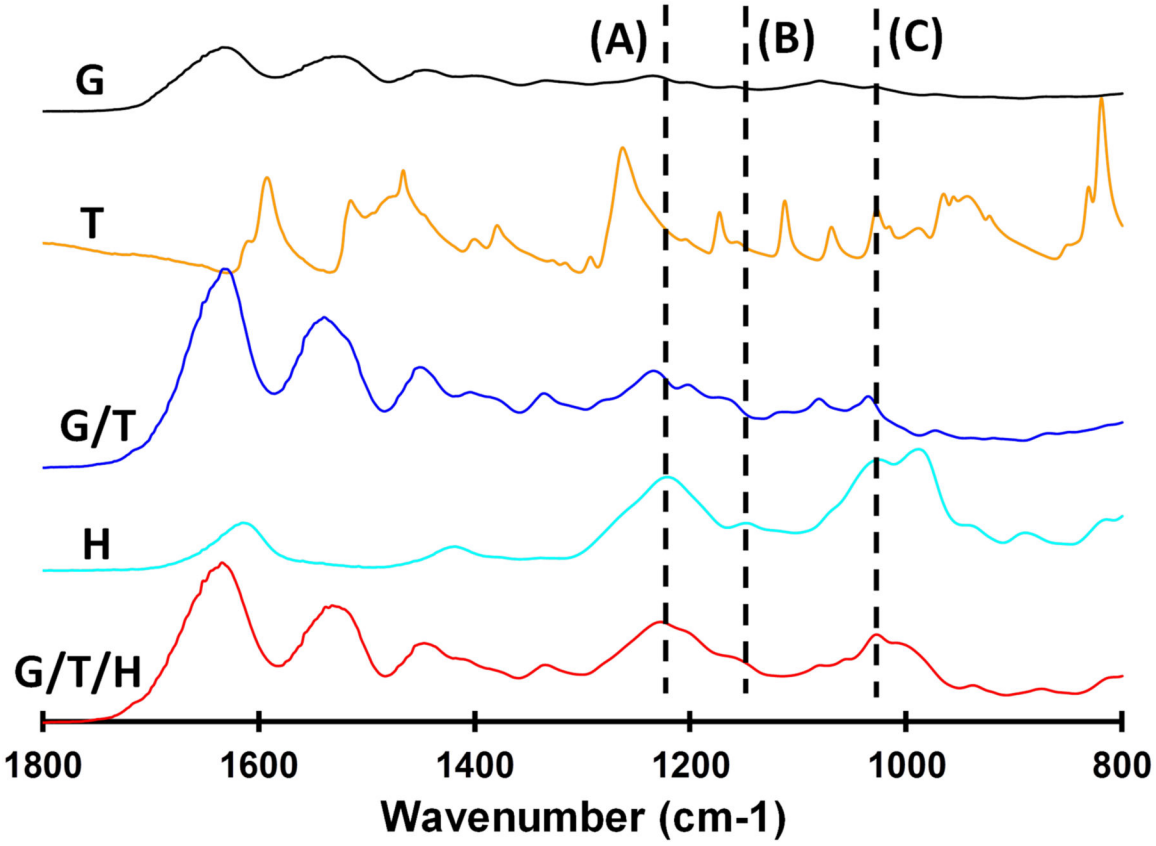

Fig 3.

FTIR spectroscopy of (**a**) gelatin (G); (**b**) tyramine (T); (c) gelatin/tyramine (G/T); (**d**) heparin, and (**e**) gelatin/tyramine/heparin composite scaffold (G/T/H).

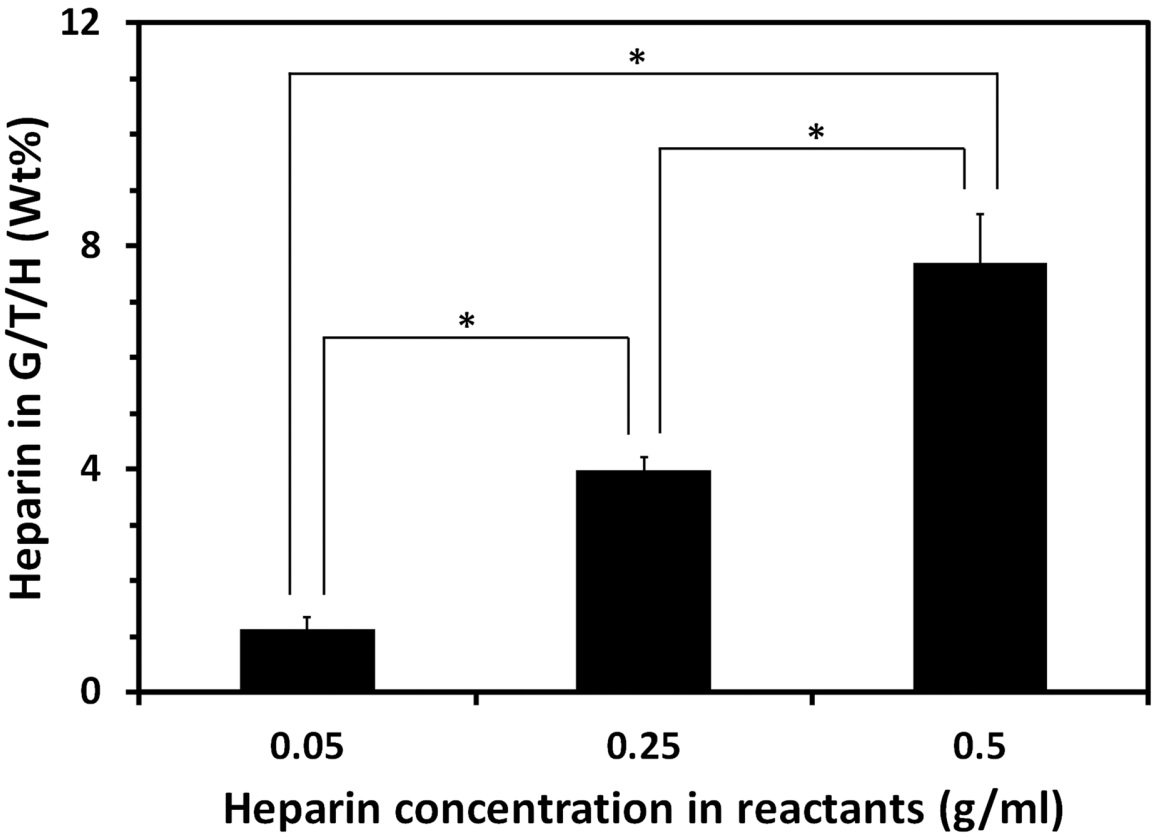

Fig 4.

Heparin content in the G/T/H using different concentrations of heparin in the reactants. * denotes $p<0.05$.

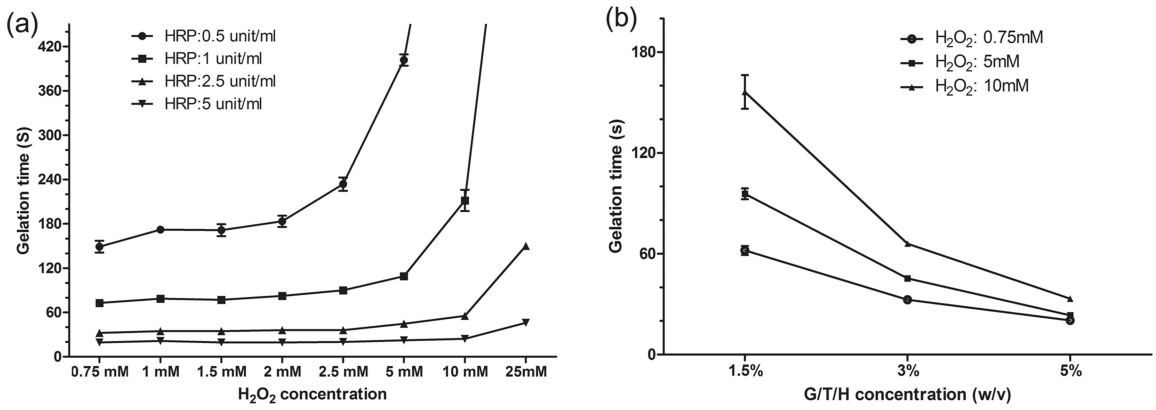

Fig 5.

Gelation time of G/T/H hydrogel as a function of HRP/H_2O_2 and G/T/H concentration. (**a**) Effect of H_2O_2 and HRP concentration on the gelation rate. G/T/H had a concentration 1.5 wt%. (**b**) Effect of G/T/H and H_2O_2 concentration on the gelation rate. HRP had a concentration of 1 unit/ml. Values represent the mean (n=3) and standard deviation.

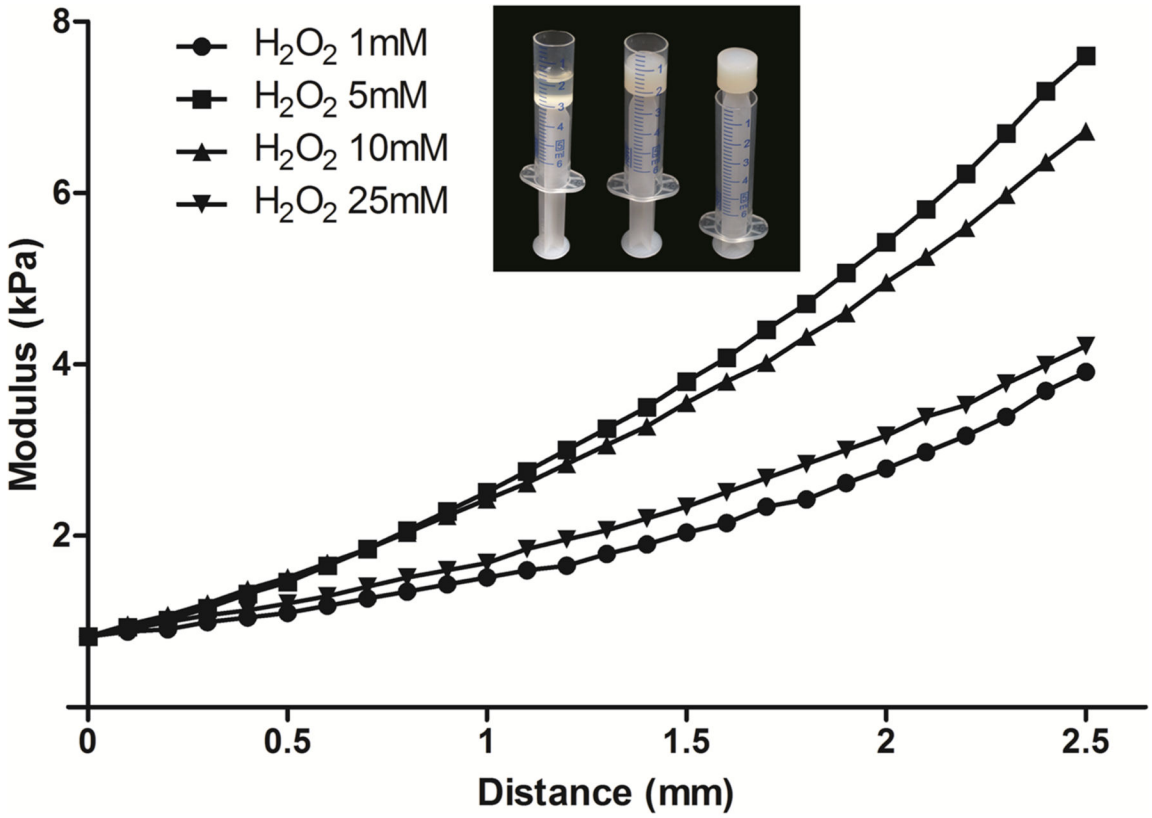

Fig 6.

Storage modulus of the G/T/H hydrogel at different H_2O_2 concentrations as a function of distance. The concentrations of G/T/H and HRP were fixed at 5 wt% and 1 unit/ml, respectively. Insets were the images of the G/T/H before and after gelation in a 5 ml syringe with the top barrel cut off. In the X-axis, the initial position of the gel was defined as the distance of 0 mm).

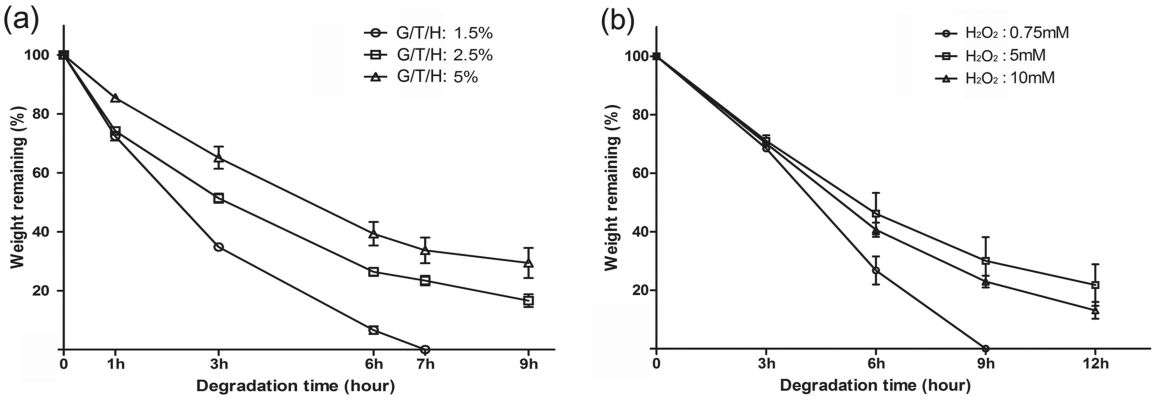

Fig 7.

In vitro degradation of G/T/H hydrogels after incubation in PBS in the presence of collagenase (10 unit/ml) at 37°C (**a**) Effect of the G/T/H concentration on degradation rate. The concentrations of HRP and H_2O_2 were fixed at 1 unit/ml and 5 mM, respectively. (**b**) Effect of the H_2O_2 concentration on degradation rate. The concentrations of G/T/H and HRP were fixed at 5 wt% and 1 unit/ml, respectively. Values represent the mean (n=3) and standard deviation.

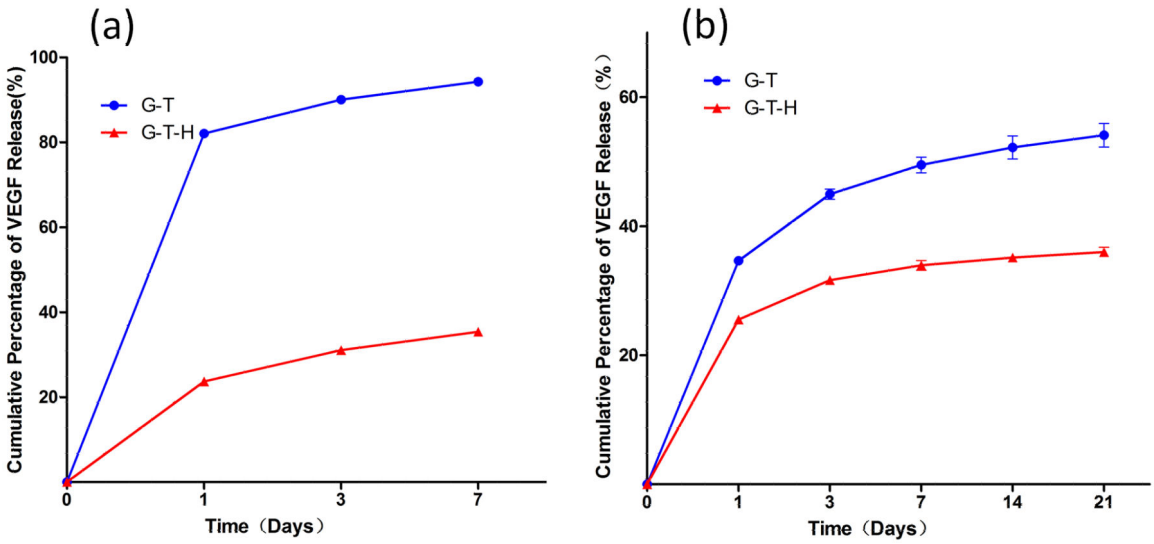

Fig 8.

Cumulative release of VEGF from the G/T hydrogels [●] and the G/T/H hydrogels [▲] using (**a**) the absorption method; and (**b**) the physically entrapped method.

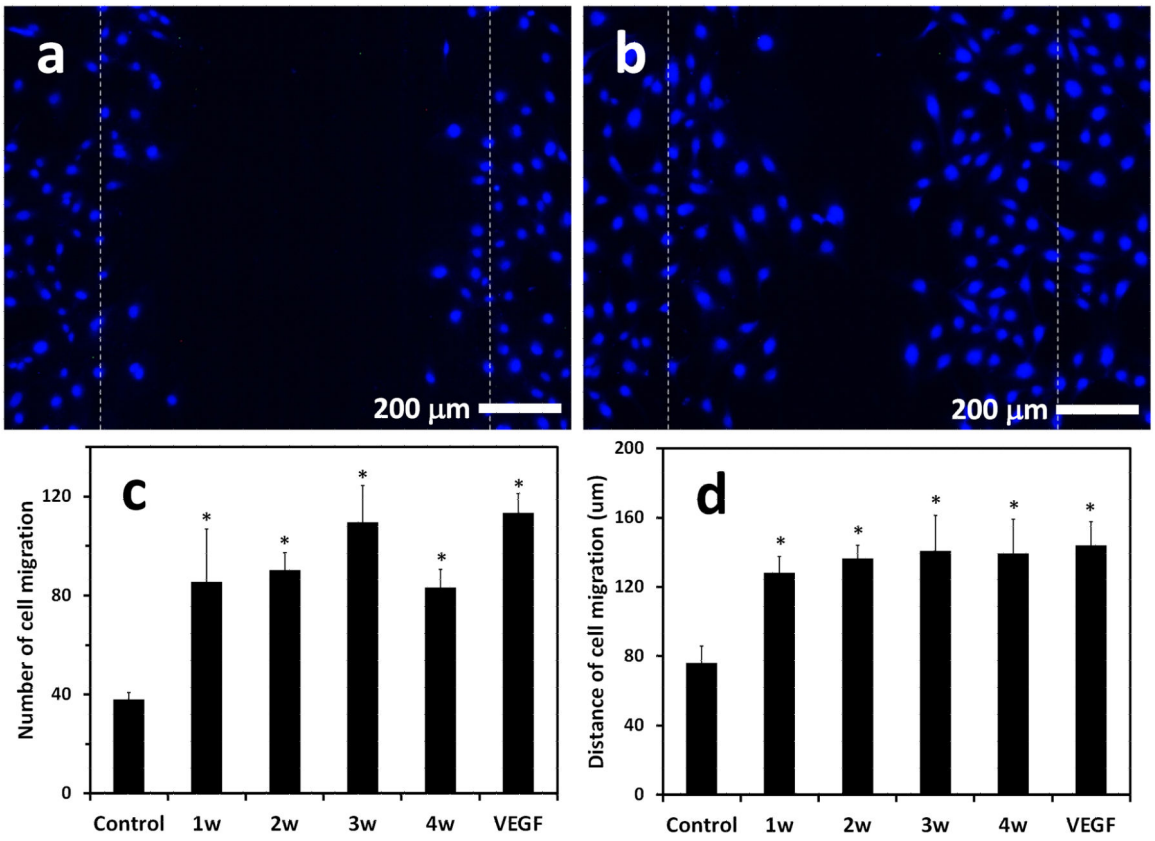

Fig 9.

Effect of released VEGF in HUVECs on migration assays. HUVECs were cultured for 24 h in (**a**) EGM-2 basal medium and (**b**) EGM-2 basal medium in the presence of released VEGF that was collected at 1 week from the VEGF-loaded G/T/H hydrogel. Scratch migration assay was performed and Hoechst-33342-stained nuclei migrating into the scratched region were shown. Quantification of the (**c**) cell number and (**d**) cell distance that migrated into the wounded area by treating with EGM-2 basal medium and EGM-2 basal medium in the presence of released VEGF (1w, 2w, 3w and 4w) from the VEGF-loaded G/T/H. Scale bar indicates 200 μm. Values are represented as mean ± SEM; *$p < 0.05$ *vs*. control.

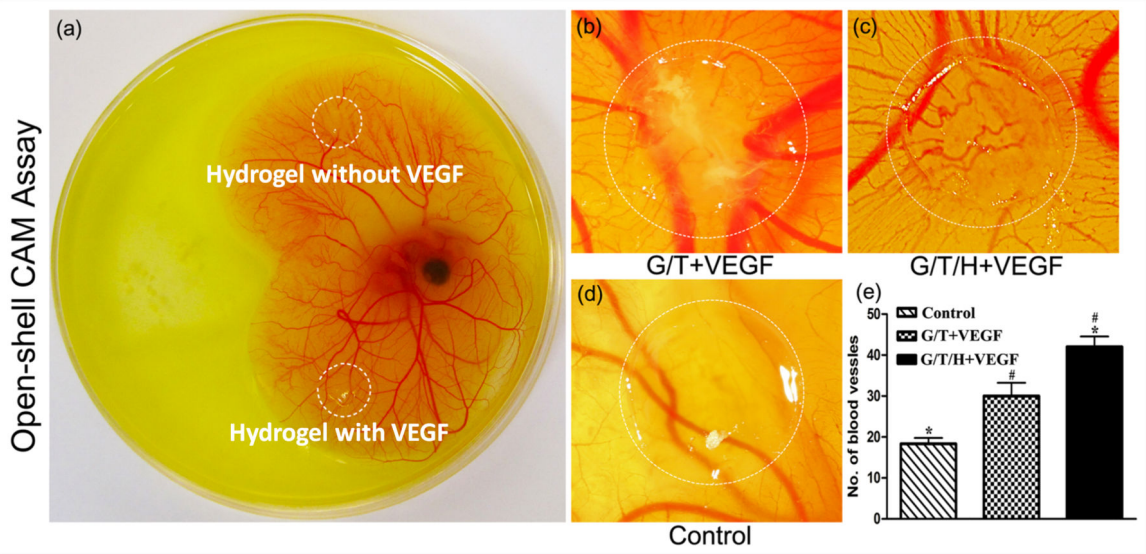

Fig 10.

Bioactivity of the released VEGF from the VEGF-loaded G/T/H hydrogels using a chorioallantoic membrane (CAM) assay. (**a**) Hydrogels loaded with 1μg of VEGF and without VEGF were placed on chicken embryo CAM (E8) (**b**) 2.5 wt% G/T hydrogel loaded with 1μg VEGF after 5 days of incubation. (**c**) 2.5 wt% G/T/H hydrogel loaded with 1μg VEGF after 5 days of incubation. (**d**) 2.5 wt% G/T hydrogel without VEGF after 5 days of incubation. (e) Quantification of the blood vessels surrounding the gel. Values are represented as mean ± SEM; *$p<0.01$, $^{\#}p<0.05$.

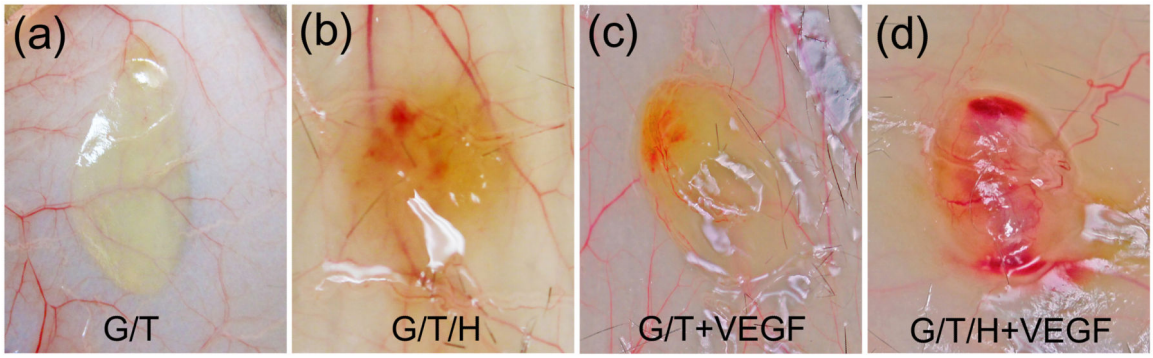

Fig 11.

Gross images of the implanted hydrogels 2 weeks after subcutaneous injection. (**a**) Gross view of the G/T hydrogel. (**b**) Gross view of the G/T/H hydrogel. (**c**) Gross view of the VEGF-loaded G/T hydrogel. (**d**) Gross view of the VEGF-loaded G/T/H hydrogel.

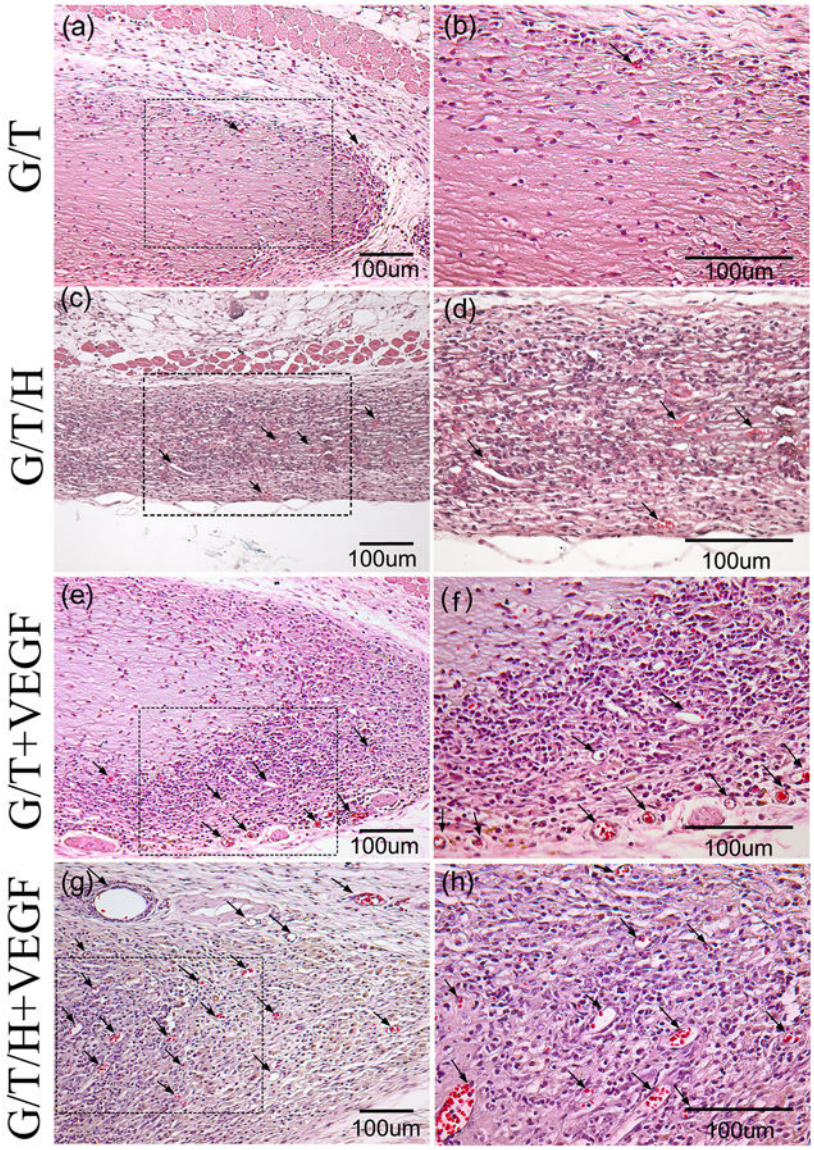

Fig 12.

H&E staining images of the G/T/H constructs after subcutaneous implantation for 2 weeks. (**a, b**) H&E staining of the G/T hydrogel. (**c, d**) H&E staining of the G/T/H hydrogel. (**e, f**) H&E staining of the VEGF-loaded G/T hydrogel. (**g, h**) H&E staining of the VEGF-loaded G/T/H hydrogel. (b), (d), (f) and (h) are high magnification images of the dotted box in (a), (c), (e) and (g), respectively. Scale bars indicate 100 μm. Arrows indicate blood vessels.

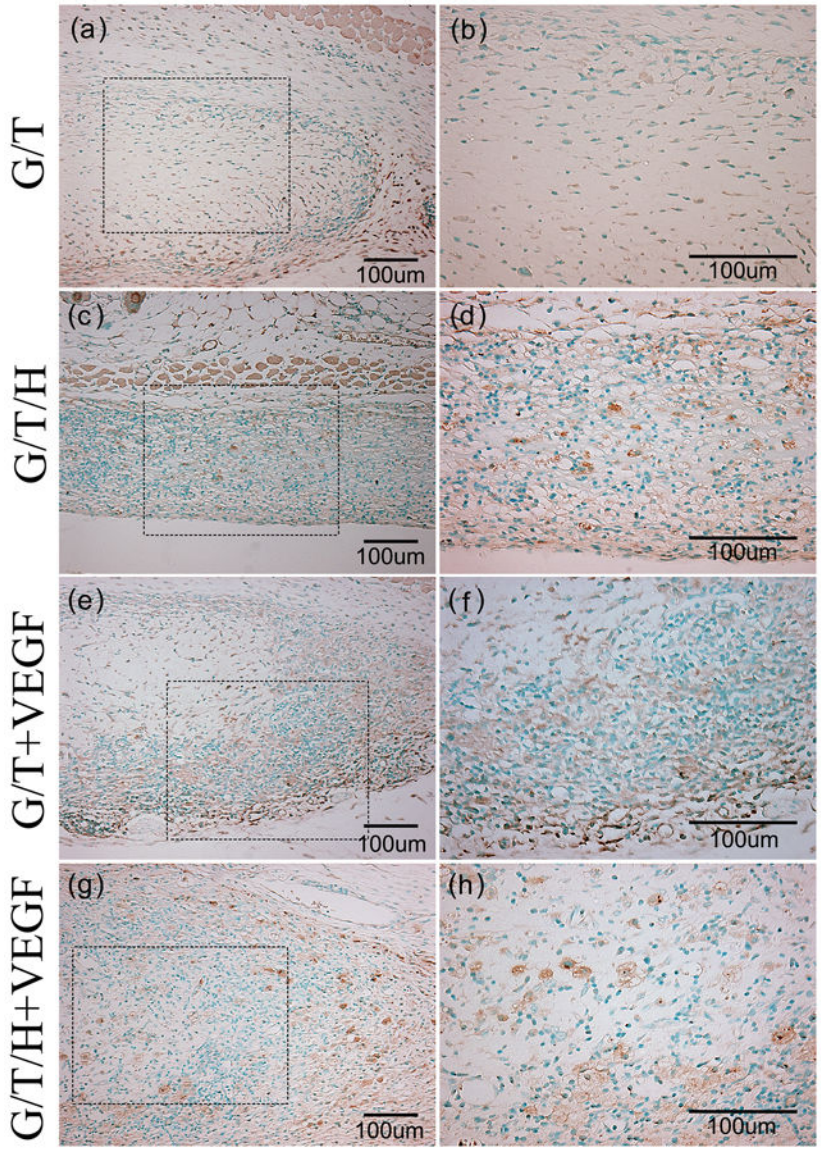

Fig 13.

α-SMA staining images of the G/T/H constructs after subcutaneous implantation for 2 weeks. (**a, b**) α -SMA staining of the G/T hydrogel. (**c, d**) α -SMA staining of the G/T/H hydrogel. (**e, f**) α -SMA staining of the VEGF loaded G/T hydrogel. (**g, h**) α -SMA staining of the VEGF loaded G/T/H hydrogel. (b), (d), (f) and (h) are high magnification images of the dotted box in (a), (c), (e) and (g), respectively. Scale bars indicate 100 μm.

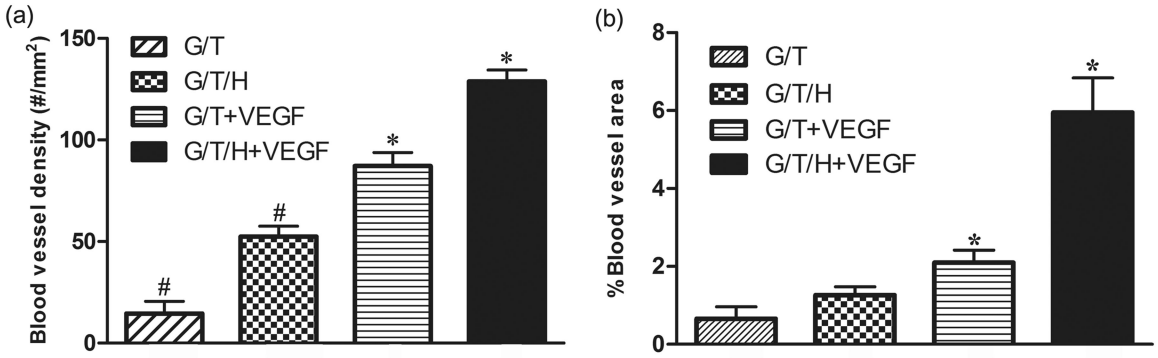

Fig 14.

The average blood vessel density (**a**) and average blood vessel area (**b**) within different kinds of hydrogels after subcutaneous implantation for 2 weeks. Values are represented as mean ± SEM; (*, #) $p<0.01$.